NeuroImage: Clinical 3 (2013) 1–7

Contents lists available at SciVerse ScienceDirect

NeuroImage: Clinical

journal homepage: www.elsevier.com/locate/ynicl

Multi-delay multi-parametric arterial spin-labeled perfusion MRI in acute ischemic stroke — Comparison with dynamic susceptibility contrast enhanced perfusion imaging ☆

Danny J.J. Wang [a,b,*], Jeffry R. Alger [a,b], Joe X. Qiao [b], Matthias Gunther [c], Whitney B. Pope [b], Jeffrey L. Saver [a], Noriko Salamon [b], David S. Liebeskind [a] for the UCLA Stroke Investigators

[a] Department of Neurology, UCLA, Los Angeles, CA, USA
[b] Department of Radiology, UCLA, Los Angeles, CA, USA
[c] Institute for Medical Image Computing, University of Bremen, Bremen, Germany

ARTICLE INFO

Article history:
Received 19 April 2013
Received in revised form 26 June 2013
Accepted 26 June 2013
Available online xxxx

Keywords:
Acute stroke
Ischemia
Arterial spin labeling (ASL)
Perfusion MRI
Dynamic susceptibility contrast (DSC)
Multi-delay
Multi-parametric

ABSTRACT

The purpose of the present study was to present a multi-delay multi-parametric pseudo-continuous arterial spin labeling (pCASL) protocol with background suppressed 3D GRASE (gradient and spin echo) readout for perfusion imaging in acute ischemic stroke. PCASL data at 4 post-labeling delay times (PLD = 1.5, 2, 2.5, 3 s) were acquired within 4.5 min in 24 patients (mean age 79.7 ± 11.4 years; 11 men) with acute middle cerebral artery (MCA) stroke who also underwent dynamic susceptibility contrast (DSC) enhanced perfusion imaging. Arterial transit times (ATT) were estimated through the calculation of weighted delays across the 4 PLDs, which were included in the calculation of cerebral blood flow (CBF) and arterial cerebral blood volume (CBV). Mean perfusion parameters derived using pCASL and DSC were measured within MCA territories and infarct regions identified on diffusion weighted MRI. The results showed highly significant correlations between pCASL and DSC CBF measurements ($r >= 0.70$, $p <= 0.0001$) and moderately significant correlations between pCASL and DSC CBV measurements ($r >= 0.45$, $p <= 0.027$) in both MCA territories and infarct regions. ASL ATT showed correlations with DSC time to the maximum of tissue residual function (Tmax)($r = 0.66$, $p = 0.0005$) and mean transit time (MTT)($r = 0.59$, $p = 0.0023$) in leptomeningeal MCA territories. The present study demonstrated the feasibility for noninvasive multi-parametric perfusion imaging using ASL for acute stroke imaging.

1. Introduction

During the past decade, arterial spin labeled (ASL) perfusion MRI has undergone several technical advances including higher magnetic fields, more efficient spin labeling and image acquisition schemes which facilitated its translation into clinical neuroimaging (Detre et al., 2012). It is now feasible to apply ASL for perfusion imaging in acute ischemic stroke (AIS). Several recent studies have evaluated the clinical utility of ASL in AIS through comparison with the reference standard of dynamic susceptibility contrast (DSC) enhanced perfusion weighted imaging (PWI) (Bokkers et al., 2012; Hernandez et al., 2012; Wang et al., 2012; Zaharchuk et al., 2012). These studies showed that ASL is largely consistent with DSC for detecting/delineating hypoperfused brain regions, although ASL may miss small lesions and may overestimate perfusion/diffusion mismatch due to prolonged arterial transit time (ATT) in stroke. Among the multiple hemodynamic parameters generated by DSC PWI, ASL estimate of cerebral blood flow (CBF) was found to best match temporal parameters of a contrast bolus such as the mean transit time (MTT) and time to the maximum of tissue residual function (Tmax) (Wang et al., 2012).

Existing ASL studies on stroke generally employed a single post-labeling delay (PLD) time typically between 1.5 and 2 s for the estimation of CBF. Consequently, prolonged ATT greater than the PLD may result in intravascular labeled signals as well as underestimation of perfusion in brain tissue. It would be ideal to acquire serial ASL images at multiple PLDs so that both ATT and CBF can be estimated simultaneously (Gunther et al., 2001; MacIntosh et al., 2010). Such a multi-delay ASL approach has several potential advantages over existing single delay ASL scans, including improved accuracy of CBF quantification, imaging of multiple hemodynamic parameters (ATT, CBF and arterial cerebral blood volume or aCBV), and better visualization of

* Corresponding author at: Department of Neurology, University of California Los Angeles, 660 Charles E Young Dr South, Los Angeles, CA 90095, USA. Tel.: +1 310 983 3667; fax: +1 310 794 7406.
E-mail address: jwang71@gmail.com (D.J.J. Wang).

2213-1582/$ – see front matter © 2013 The Authors. Published by Elsevier Inc. All rights reserved.
http://dx.doi.org/10.1016/j.nicl.2013.06.017

collateral flow through dynamic image series. The main limiting factor for such a multi-delay ASL approach has been the relatively long scan time required. This issue has recently been addressed by combining single-shot 3D GRASE (gradient and spin echo), background suppression and pseudo-continuous ASL (pCASL) which resulted in dramatic improvements in the temporal stability of ASL image series (Fernandez-Seara et al., 2008; Gunther et al., 2005). The purpose of this study was to present such a multi-delay multi-parametric pCASL protocol. Its accuracy was evaluated by comparison with DSC PWI in 24 patients with AIS. We hypothesized that multi-delay ASL CBF with correction of arterial transit effects agrees with DSC CBF, and ASL ATT is consistent with DSC Tmax and MTT measurements in AIS patients.

2. Materials and methods

2.1. Patient selection

The present analysis was performed on data collected from Dec 2011 to July 2012 in an ongoing prospective registry of patients evaluated with diffusion–perfusion MRI at our academic medical center. Image data were included in this study if: (1) the patient was diagnosed as acute middle cerebral artery (MCA) stroke, (2) baseline MRI was performed within 48 h of symptom onset, (3) both ASL and DSC perfusion imaging were performed. The UCLA Institutional Review Boards approved the study.

2.2. MRI protocols

All patients underwent MRI on Siemens 1.5 T Avanto or 3.0 T TIM Trio systems (Erlangen, Germany), using 12 channel head coils. The MRI protocol included diffusion weighted imaging (DWI), gradient recalled echo, fluid attenuated inversion recovery (FLAIR) and perfusion weighted imaging sequences. ASL scans were performed using a 4-delay pCASL protocol with background suppressed 3D GRASE readout (labeling pulse duration = 1.5 s, PLD = 1.5/2/2.5/3 s, TR = 3.5/4/4.5/5 s, FOV = 22 cm, matrix = 64 × 64, 16 × 8mm slices, rate-2 GRAPPA, TE = 22 ms, 8 pairs of tag and control for each delay, total scan time 4 min 30 s). DSC PWI scans were acquired using a gradient-echo echo-planar imaging (EPI) sequence (TR = 2.9/1.9 s, TE = 45/30 ms for 1.5/3 T, FOV = 22 cm, matrix = 128 × 128, 26 × 5mm slices, scan time = 2 min) with an intravenous bolus injection of gadolinium contrast agent (0.1 mmol/kg).

2.3. Post-processing of ASL and DSC PWI

Data analysis was performed with Interactive Data Language (IDL (Boulder, CO, USA)) software programs developed in-house. ASL images were corrected for motion, pairwise subtracted between label and control images followed by averaging to generate the mean difference image, $\Delta M(i)$, for each PLD respectively. A weighted delay, *WD*, was calculated by Eq. (1) and converted into ATT (δ) based on the theoretical relationship between *WD* and ATT (Dai et al., 2012)

$$WD = \left[\sum_{i=1}^{4} w(i)\Delta M(i)\right] \Big/ \left[\sum_{i=1}^{4} \Delta M(i)\right] \quad (1)$$

where $w(i)$ is the PLD (=1.5/2/2.5/3 s). The estimation of ATT based on *WD* through a monotonic function provided a robust solution for pCASL data with 4 PLDs in stroke (see Supplemental Fig. 1 for methodological details). CBF at each delay, $f(i)$, was then calculated by

$$f(i) = \frac{\lambda \Delta M(i) R_{1a}}{2\alpha M_0 [\exp((\min(\delta - w(i), 0) - \delta) R_{1a}) - \exp(-(\tau + w(i)) R_{1a})]} \quad (2)$$

where R_{1a} (=0.72/0.61 s^{-1} at 1.5/3 T) is the longitudinal relaxation rate of blood, M_0 is the equilibrium magnetization of brain tissue, α (=0.8) is the tagging efficiency, τ (=1.5 s) is the duration of the labeling pulse, and λ (=0.9 g/ml) is blood/tissue water partition coefficient. The final CBF was the mean of the estimated CBF at each PLD. Arterial CBV (aCBV) map was generated by the product of ATT and mean CBF of 4 PLDs, which indicates the arterial blood volume from the labeling plane to the imaging voxel.

$$\text{aCBV} = \text{CBF} \cdot \text{ATT}. \quad (3)$$

Fig. 1 illustrates the post-processing steps for a representative 4-delay pCASL dataset collected in a patient with left MCA stroke. Labeled signal did not appear in the affected region until the PLD reached 2.5 s (arrows), leading to prolonged ATT in the left MCA territory. CBF and aCBV maps were subsequently generated by substituting ATT into Eqs. (2) and (3) respectively, which showed hypoperfusion in the affected left MCA territory.

DSC images were corrected for head motion, followed by deconvolution of the image series with the arterial input function to generate multi-parametric perfusion maps including CBF, CBV, Tmax and MTT. CBF values were calculated based on the value at Tmax of the tissue residual function (R(t)) derived using block-circulant singular value decomposition (bcSVD) (Wu et al., 2003). In each case, all structural, diffusion and perfusion images were aligned using SPM8 (Wellcome Department of Cognitive Neurology, UCL, UK). ASL and DSC perfusion images were further normalized into the Montreal Neurological Institute (MNI) template space using SPM8. Subsequently, segmentation of ASL and DSC perfusion images into major vascular territories was performed using an automated region-of-interest (ROI) analysis based on a published template of vascular territories in both hemispheres (Tatu et al., 1998). The vascular territories studied included leptomeningeal and lenticulostriate (perforator) MCA. In addition, the infarction core was defined as apparent diffusion coefficient value $<550 \times 10^{-6}$ mm^2/s on DWI (Nael et al., 2013). A contralateral region-of-interest (ROI) was generated by mirroring the infarct ROI on normalized DWI in each patient.

2.4. Statistical analysis

Statistical analysis was performed using STATA 10.0 software (College Station, TX, USA). Mean ASL and DSC perfusion parameters were extracted from left and right MCA territories as well as from infarct ROIs and the contralateral mirror ROIs. An asymmetry ratio was calculated as (contralateral–ipsilateral) / (contralateral + ipsilateral) for each of the perfusion parameters in ASL and DSC PWI (MacIntosh et al., 2010). The rationale for using asymmetry ratio for the comparison of ASL and DSC was to minimize the variability in absolute quantification of perfusion parameters between the two modalities. Pearson correlation coefficients were calculated between asymmetry ratios of ASL and DSC for each of the perfusion parameters respectively. Pearson correlation coefficients were also calculated between asymmetry ratios of ASL and DSC perfusion parameters and NIH Stroke Scale (NIHSS) scores. Partial correlation analyses were carried out between ASL and DSC by including NIHSS and/or field strength as covariates. Paired *t*-test was applied for comparing quantitative CBF values in MCA territories and infarct ROIs derived using 4 PLDs and a single PLD of 2 s (Qiu et al., 2012). The significance level was defined as $p \leq 0.05$ (2-sided).

3. Results

3.1. Demographic and clinical information

Image data from 24 patients (mean age 79.7 ± 11.4 years; 11 men) with acute MCA ischemic stroke were included. NIHSS scores ranged from 1 to 36, with a median of 16.5. The median time from stroke onset to imaging was 4.7 h (range 1.6 to 38.3 h). Half of the 24 patients were scanned on 1.5 T and another half on 3 T. Demographic and

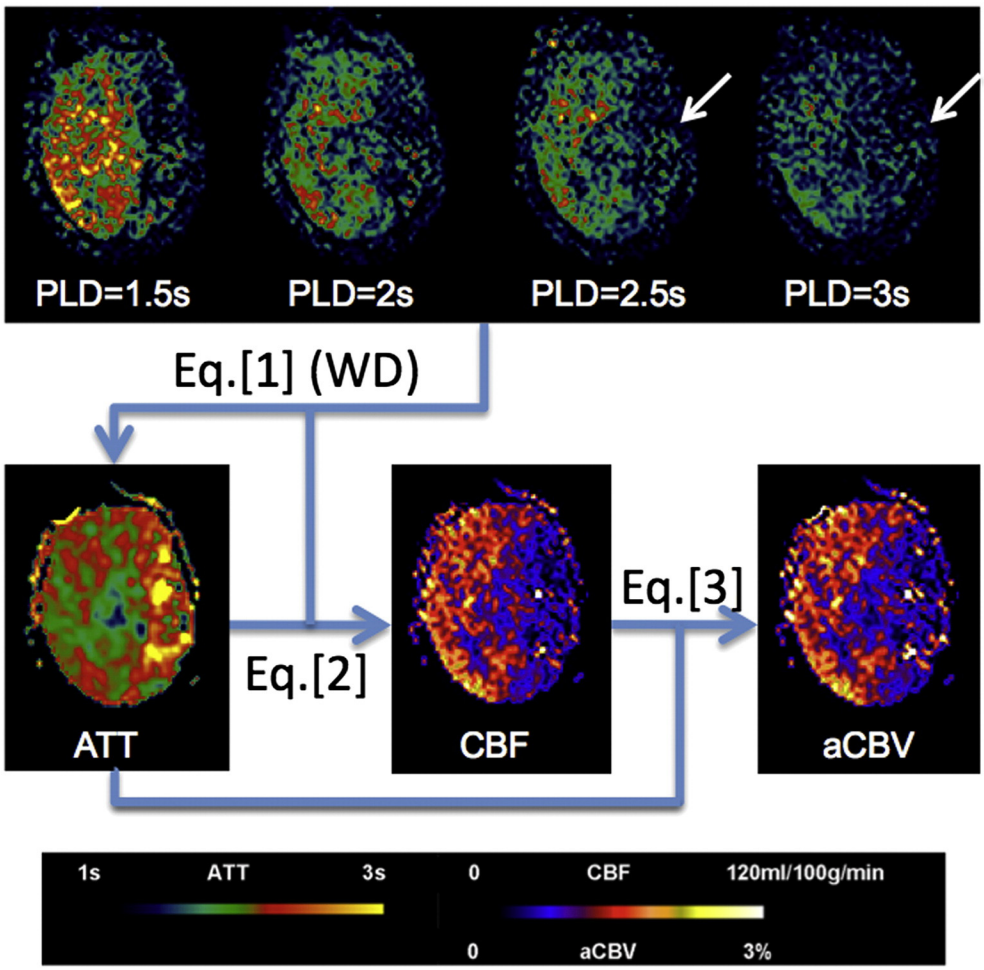

Fig. 1. Diagram of post-processing steps for a representative 4-delay pCASL dataset collected in a 61-year old female patient (case #15) with left MCA stroke. Labeled signal only appears in affected region when the PLD reaches 2.5 s (arrows), leading to prolonged ATT in the left MCA territory. CBF at each PLD is calculated by substituting ATT into Eq. (2) followed by averaging to generate the mean CBF map. The product of mean CBF and ATT provides aCBV map.

clinical information of the 24 stroke patients are provided in Supplemental Table 1.

3.2. Quantitative MCA territory analysis

Table 1 lists the Pearson correlation coefficients between 4-delay pCASL and DSC asymmetry ratios of multiple perfusion parameters. There were highly significant correlations between pCASL and DSC asymmetry ratios of CBF measurements in both leptomeningeal ($r = 0.74$, $p < 0.0001$) and perforator MCA ($r = 0.73$, $p = 0.0001$) territories. The correlation coefficients were slightly reduced between pCASL CBF acquired at the single PLD of 2 s ($r = 0.72$ and 0.71, $p = 0.0001$) and DSC CBF. PCASL aCBV measurements were significantly correlated with DSC CBV measurements in both leptomeningeal ($r = 0.57$, $p = 0.0034$) and perforator MCA ($r = 0.58$, $p = 0.0028$) territories. PCASL estimation of ATT, however, was significantly correlated with DSC Tmax ($r = 0.66$, $p = 0.0005$) and MTT ($r = 0.59$, $p = 0.0023$) in the leptomeningeal but not perforate MCA territory.

Figs. 2, 3 and 4 show 3 representative stroke cases with prolonged ATT around the infarct region in all 3 cases, well matching DSC results. CBF around the ischemic lesion using 4-delay pCASL was slightly increased compared to CBF using a single PLD of 2 s. The mean and

Table 1
Pearson correlation coefficients (and p values) between asymmetry ratios of ASL and DSC perfusion parameters in leptomeningeal and perforator MCA territories as well as in infarct and contralateral mirror ROIs.

Pearson correlation coefficients	ASL CBF vs. DSC CBF	ASL CBF 2 s vs. DSC CBF	ASL aCBV vs. DSC CBV	ASL ATT vs. DSC Tmax	ASL ATT vs. DSC MTT
Leptomeningeal MCA	0.74** ($p < 0.0001$)	0.72** ($p = 0.0001$)	0.57** ($p = 0.0034$)	0.66** ($p = 0.0005$)	0.59** ($p = 0.0023$)
Perforator MCA	0.73** ($p = 0.0001$)	0.71** ($p = 0.0001$)	0.58** ($p = 0.0028$)	0.28 ($p = 0.18$)	0.12 ($p = 0.59$)
Infarct ROI	0.70** ($p = 0.0001$)	0.70** ($p = 0.0001$)	0.45* ($p = 0.027$)	0.18 ($p = 0.39$)	−0.14 ($p = 0.52$)

** $p < 0.005$.
* $p < 0.05$.

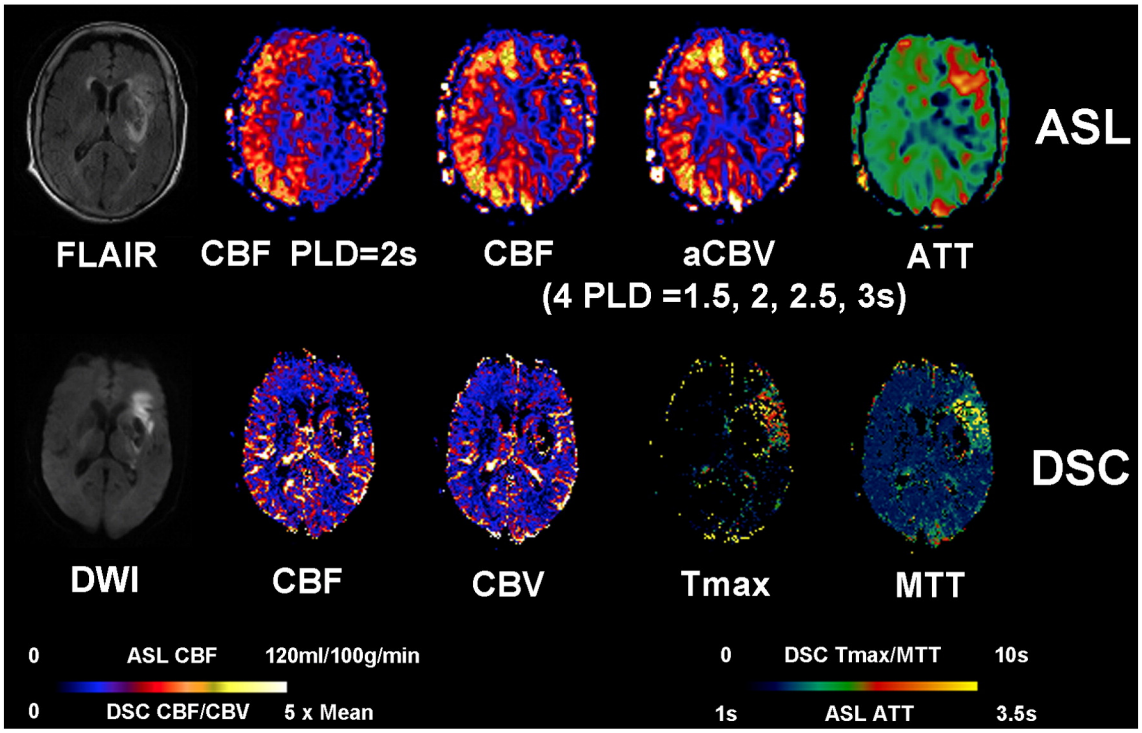

Fig. 2. Representative AIS case with aligned FLAIR, DWI, multiparametric ASL and DSC PWI. An 89-year-old female (case #11) with a history of atrial fibrillation and hypertension was admitted to ER after being found down unconsciously and was found to have a left MCA stroke with a Baseline NIHSS of 20. The patient was scanned 8.1 h after the onset before receiving any endovascular treatment. Restricted diffusion and FLAIR hyperintensities were seen in the left basal ganglia, internal capsule and left frontal lobe. ASL shows decreased CBF, decreased CBV and prolonged ATT in the left MCA region. DSC Tmax and MTT were prolonged in the left frontal region with mildly decreased CBF and CBV.

standard deviation (SD) of CBF values in the affected (ipsilateral) and contralateral MCA territories are listed in Table 2. PCASL CBF values generated using 4 PLDs were increased by 1–2 ml/100 g/min compared to CBF values acquired using a single PLD of 2 s ($p < 0.05$) in affected MCA territories, while no significant differences were detected in contralateral MCA territories ($p > = 0.062$).

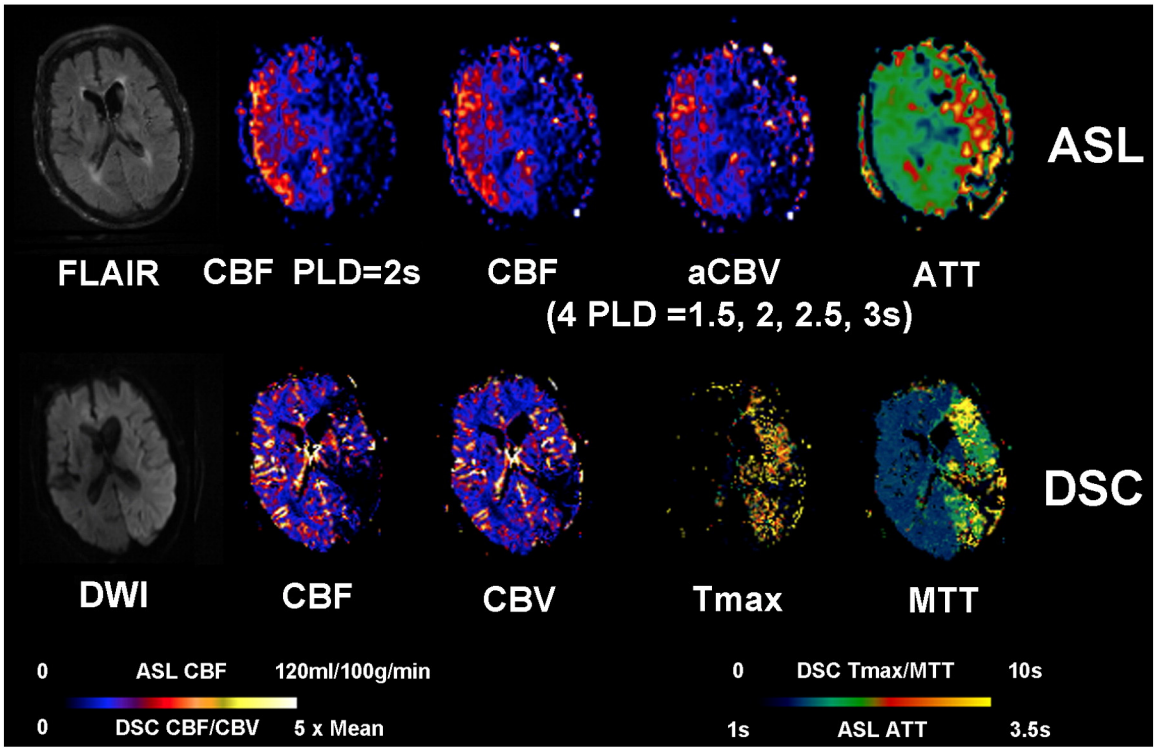

Fig. 3. A 94-year-old male (case #13) with a unclear past medical history presented with aphasia, right-sided numbness and weakness and was found to have a left MCA stroke with a Baseline NIHSS of 24. IV tPA was given before the patient was scanned 1.6 h after the onset. Acute restricted diffusion is present throughout the left parietal, temporal, and occipital lobes, as well as the left caudate head and body. ASL shows decreased CBF, decreased CBV and prolonged ATT in the left MCA region. DSC Tmax and MTT were prolonged in the left MCA region with decreased CBF and CBV.

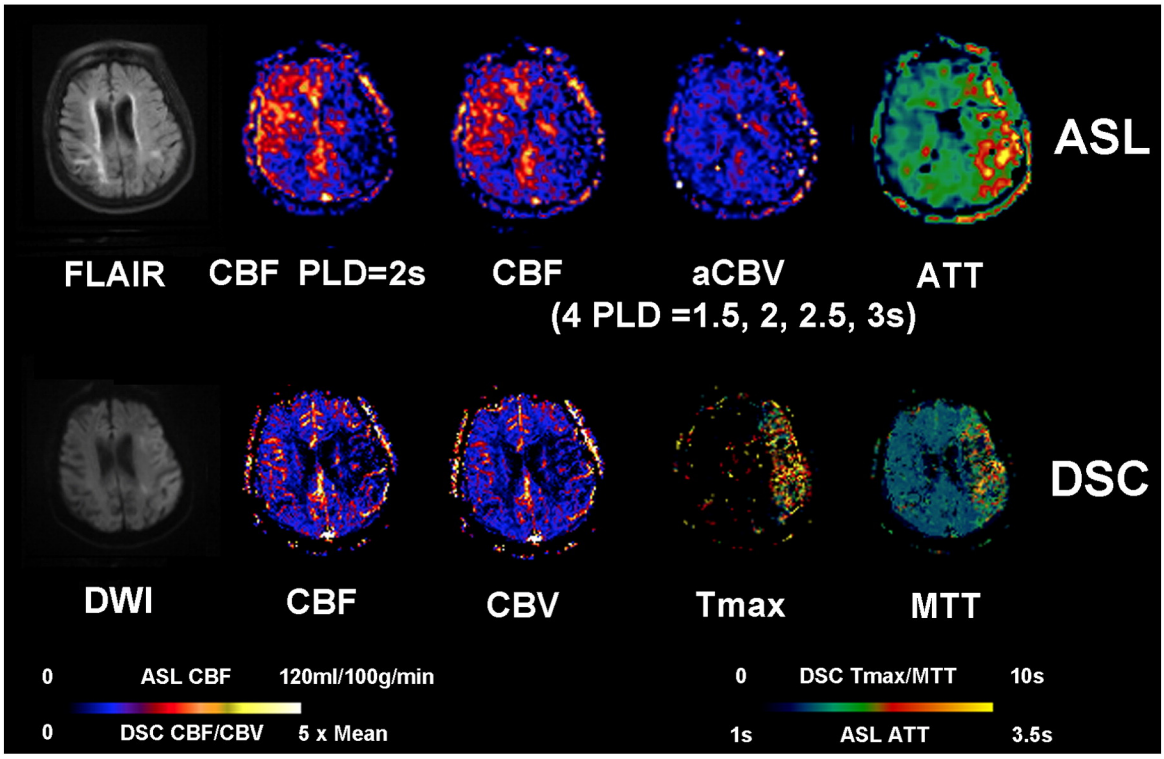

Fig. 4. An 85-year-old female (case #14) with a past medical history significant for paroxysmal atrial fibrillation, presented with aphasia, right-sided weakness and a baseline NIHSS of 19. IV tPA was given before the patient was scanned 2.5 h after the onset. Restricted diffusion is present throughout the left MCA territory with T2/FLAIR hyperintensity. ASL shows decreased CBF, decreased CBV and prolonged ATT in the left MCA region. DSC-Tmax and MTT were prolonged in the left MCA region with mildly decreased DSC-CBF and CBV.

3.3. Quantitative infarct region analysis

As shown in Table 1, within infarct ROIs identified on DWI and their contralateral mirror ROIs, pCASL measurements of asymmetry ratios of CBF ($r = 0.70$, $p = 0.0001$) and aCBV ($r = 0.45$, $p = 0.027$) were significantly correlated with DSC CBF and CBV measurements respectively. PCASL CBF measurements at the single PLD of 2 s were similarly correlated with DSC CBF ($r = 0.70$, $p = 0.0001$). However, there were no significant associations between pCASL ATT and DSC Tmax or MTT within infarct ROIs (see Table 1).

Fig. 5 shows an AIS case with a severe (or "malignant") infarction on the right MCA territory (infarct volume = 222 ml, NIHSS = 18). While the hypoperfused lesion was apparent on ASL CBF and aCBV maps, the estimated ATT was only prolonged in the right frontal region, but was normal or even reduced in the right MCA territory. As a result, ASL ATT did not correlate with DSC Tmax or MTT in infarct ROIs in the cohort of 24 stroke patients. The mean asymmetry ratio of ATT (-0.076 ± 0.094) was significantly smaller (in terms of magnitude) than that of Tmax (-0.39 ± 0.35, $p = 0.0001$). As shown in Table 2, the use of 4 PLDs did not significantly alter CBF values in infarct and mirror ROIs compared to the use of a single PLD of 2 s. However, the mean asymmetry ratio of CBF was reduced by the use of 4 PLDs (from 0.41 ± 0.25 to 0.37 ± 0.21, $p = 0.036$). Note the mean asymmetry ratio of ATT (-0.076 ± 0.094) was significantly less than 0, suggesting prolonged ATT in infarct lesions compared to the contralateral hemisphere ($p = 0.0003$).

3.4. Correlation with NIHSS

Significant correlations with NIHSS scores were found using ASL and DSC perfusion measurements in infarct ROIs but not in MCA territories (see Supplemental Table 2). PCASL CBF using 4 PLDs and single PLD of 2 s as well as aCBV measurements were correlated with NIHSS ($r >= 0.46$, $p <= 0.025$). DSC CBF and CBV measurements were also correlated with NIHSS ($r = 0.68$, $p = 0.003$). However, no associations were detected between temporal parameters using pCASL or DSC PWI and NIHSS. Partial correlation analyses between ASL and DSC by including NIHSS as a covariate did not affect the general relationship between ASL and DSC (see Supplemental Table 3), except that there was a reduction of correlation coefficients in infarct ROIs (since NIHSS was significantly correlated with ASL and DSC CBF).

Table 2
Mean ± SD of CBF values and associated asymmetry ratios (AR) in leptomeningeal and perforator MCA territories as well as in infarct and contralateral mirror ROIs.

CBF (ml/100 g/min)	ASL CBF (4 PLDs)		ASL CBF (PLD = 2 s)		AR CBF (4 PLDs)	AR CBF (PLD = 2 s)
	Ipsilateral	Contralateral	Ipsilateral	Contralateral		
Leptomeningeal MCA	29.71 ± 15.79 ($p = 0.045$)*	31.16 ± 14.21 ($p = 0.16$)	28.32 ± 16.60	30.37 ± 15.38	0.056 ± 0.30 ($p = 0.28$)	0.065 ± 0.35
Perforator MCA	27.72 ± 14.23 ($p = 0.040$)*	28.74 ± 12.64 ($p = 0.062$)	25.72 ± 16.65	27.17 ± 13.62	0.031 ± 0.24 ($p = 0.23$)	0.044 ± 0.29
Infarct ROI	20.11 ± 10.95 ($p = 0.11$)	41.01 ± 16.11 ($p = 0.27$)	18.71 ± 13.30	40.29 ± 17.90	0.37 ± 0.21 ($p = 0.036$)*	0.41 ± 0.25

* $p < 0.05$ paired *t*-test (2-sided) between CBF measurements using 4 PLDs and a single PLD of 2 s.

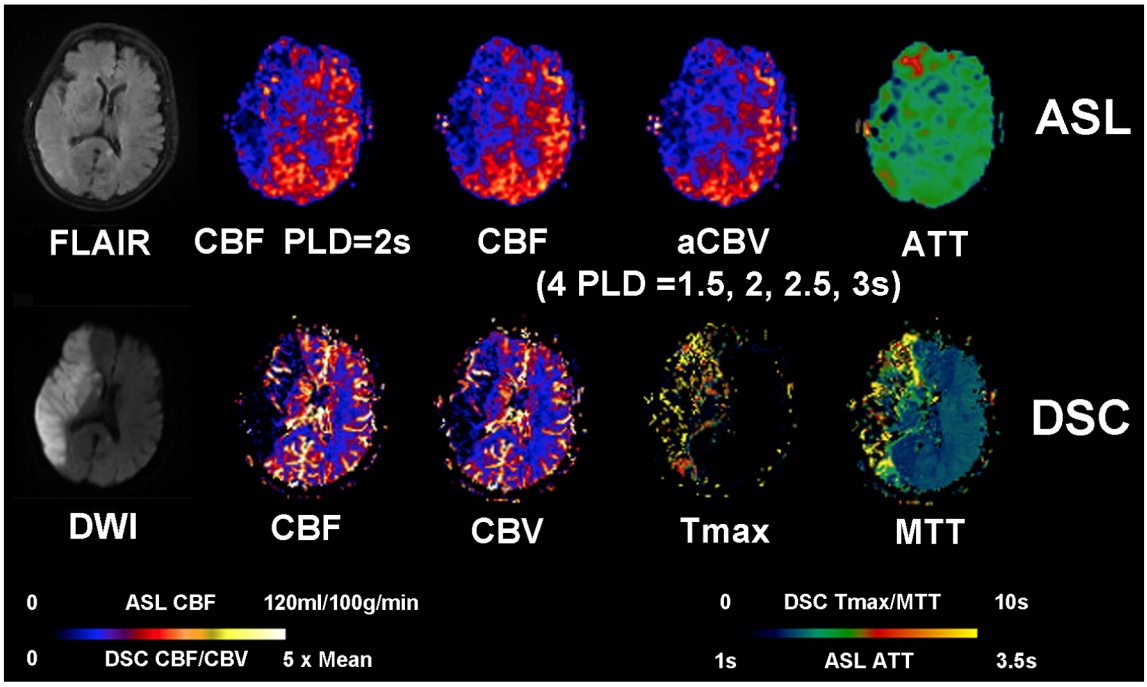

Fig. 5. An 88-year-old female (case #22) with history of hypertension presented with left-sided numbness and weakness, gait disturbance, limb ataxia, and altered mental status. The baseline NIHSS on admission was 18. Clot retrieval was performed before the patient was scanned 22.5 h after the onset. There is a large area of restricted diffusion involving the entire right MCA territory with T2/FLAIR hyperintensity. ASL shows decreased CBF and CBV in the right MCA region. However, ATT is not or only slightly prolonged in right MCA territory. DSC-Tmax and MTT were prolonged in the right MCA region with decreased DSC-CBF and CBV.

4. Discussion

The present study demonstrated the feasibility of a 4-delay pCASL GRASE protocol in a cohort of 24 MCA stroke patients. Past attempts for multi-delay multi-parametric perfusion imaging in stroke using ASL have been hampered by the relatively long scan time, low SNR, and unstable results using nonlinear least square fitting. The proposed pCASL protocol addressed these issues by a combined use of pCASL with background suppressed 3D GRASE (to shorten imaging time and improve SNR), along with a robust method for estimating ATT based on weighted delay (Dai et al., 2012). The advantage of the proposed multi-delay pCASL protocol is that multiple perfusion parameters (ATT, CBF, and aCBV) can be simultaneously estimated within 5 min scan time that would be normally required for a single delay ASL scan. Because the estimated CBF is the mean of ATT adjusted CBF at 4 PLDs, there should be a minimal penalty in SNR compared to pCASL scans performed at a single PLD, assuming the same amount of scan time.

A comparison of multi-delay pCASL and DSC PWI showed an overall high correlation between CBF measurements using the 2 modalities within MCA territories and infarct ROIs. This observation adds to the existing literature on the consistency between ASL and DSC PWI in the evaluation of AIS (Bokkers et al., 2012; Hernandez et al., 2012; Nael et al., 2013; Wang et al., 2012; Zaharchuk et al., 2012) and cerebrovascular disorders (Wolf et al., 2003). PCASL measurements of ATT, however, were significantly correlated with DSC Tmax and MTT within leptomeningeal MCA territories but not in perforator MCA or infarct ROIs. There may be 2 potential reasons for this discrepancy: 1) the size of the perforator MCA territory (10 ml) or infarct ROIs (41 ± 58 ml) was much smaller than that of leptomeningeal MCA territory (210 ml). It has been reported that pCASL has limited sensitivity for detecting small ischemic lesions due to lower spatial resolution and SNR compared to DSC PWI (Bokkers et al., 2012). 2) For severe or "malignant" infarction, the transit time may be longer than 3 s. Limited by T1 relaxation of the label, ATT could not be accurately estimated in these cases and perfusion will be underestimated. Another caveat in comparing temporal parameters of ASL and DSC is that ATT measures the time for the labeled arterial blood to flow into brain tissue, while Tmax indicates the delay in the arrival of (local) contrast bolus and MTT indicates the duration for the bolus to flow from the arterial end to the venous end. Conceptually, ATT is rather similar to Tmax than MTT which is supported by our experimental data (see Table 1).

Another interesting finding from the present study is that the 4-delay pCASL CBF calculated by taking into account ATT only showed slight improvement compared to CBF acquired at the PLD of 2 s — on average 1–2 ml/100 g/min increase in affected MCA territories. The choice for using the PLD of 2 s as the benchmark was based on recent ASL studies on cerebrovascular disorders and stroke (Qiu et al., 2012; Wang et al., 2012). The results indicated that both pCASL CBF measurements using 4 PLDs or a single PLD of 2 s are highly consistent with DSC CBF within vascular territories or infarct regions. Both pCASL and DSC CBF measurements within infarct ROIs were also correlated with NIHSS scores across the 24 stroke patients. The single delay pCASL scan, which only takes approximately 1 min to acquire, may be advantageous for perfusion imaging in AIS if CBF is the primarily parameter of interest and where scan time is limited. The 4-delay pCASL protocol, on the other hand, offers additional hemodynamic parameters including ATT and aCBV which may be more sensitive than CBF for characterizing chronic stroke (MacIntosh et al., 2010) and brain tumor (Law et al., 2006).

A less exploited parameter in the present study is aCBV which is a hemodynamic parameter describing the interaction effect between CBF and ATT. Dynamic ASL image series can also be used for the evaluation of collateral flow in AIS. Collateral flow may sustain brain tissue for hours after the occlusion of major arteries to the brain, and the augmentation or maintenance of collateral flow is therefore a potential therapeutic target (Bokkers et al., 2012; Hernandez et al., 2012). Delayed arterial transit effects characterized by focal intravascular signals and low tissue perfusion in ASL images may indicate the status of collateral perfusion (Chalela et al., 2000; Chen et al., 2009; Zaharchuk, 2011). So far, the identification of delayed transit effects and the inference of collateral perfusion have been mainly based on "snap-shot" ASL images acquired at a single PLD, typically between

1.5 and 2 s. The proposed multi-delay pCASL approach should provide improved visualization of collateral flow in AIS through dynamic image series, and the potential for quantitative assessment of collateral perfusion. Multi-delay pCASL is also advantageous for differentiating delayed transit effects and hyperemic responses, both may appear as hyper-intensities on ASL images but have different temporal profiles. These are research topics to be pursued in future studies.

This study has several limitations. The sample size is relatively small but represented a relatively uniform cohort of patients with acute MCA ischemic stroke. The choice of 4 PLDs from 1.5 to 3 s in the pCASL protocol was based on an empirical assumption that the transit time is longer than 1.5 s in stroke patients. However, a reliable perfusion cannot be estimated accurately using the present pCASL protocol if ATT is greater than 3 s. Half of the 24 patients were scanned at 1.5 T with lower SNR compared to 3 T, although including field strength as a covariate did not affect the observed relationship between ASL and DSC. Eight pairs of label and control acquisitions were performed for each PLD, resulting in reduced SNR for long PLDs. In the future, the number of acquisitions for each delay should be adjusted to compensate for the loss of SNR at long PLDs.

5. Conclusion

A multi-delay multi-parametric pCASL protocol with background suppressed GRASE readout was presented and its clinical utility was evaluated by comparison with DSC PWI in 24 patients with acute MCA stroke. There were highly significant correlations between pCASL and DSC CBF measurements and moderately significant correlations between pCASL and DSC CBV measurements in both MCA territories and infarct regions. ASL ATT showed correlations with DSC Tmax and MTT in leptomeningeal MCA territories. The present study demonstrated the feasibility for noninvasive multi-parametric perfusion imaging using ASL for acute stroke imaging.

Acknowledgment

This study was supported by the US National Institutes of Health grants R01-MH080892, R01-NS081077, R01-EB014922, R01-NS077706, K23-NS054084 and P50-NS044378.

Appendix A. Supplementary data

Supplementary data to this article can be found online at http://dx.doi.org/10.1016/j.nicl.2013.06.017.

References

Bokkers, R.P., Hernandez, D.A., Merino, J.G., Mirasol, R.V., van Osch, M.J., Hendrikse, J., Warach, S., Latour, L.L., 2012. Whole-brain arterial spin labeling perfusion MRI in patients with acute stroke. Stroke; A Journal of Cerebral Circulation 43, 1290–1294.

Chalela, J.A., Alsop, D.C., Gonzalez-Atavalez, J.B., Maldjian, J.A., Kasner, S.E., Detre, J.A., 2000. Magnetic resonance perfusion imaging in acute ischemic stroke using continuous arterial spin labeling. Stroke 31, 680–687.

Chen, J., Licht, D.J., Smith, S.E., Agner, S.C., Mason, S., Wang, S., Silvestre, D.W., Detre, J.A., Zimmerman, R.A., Ichord, R.N., Wang, J., 2009. Arterial spin labeling perfusion MRI in pediatric arterial ischemic stroke: initial experiences. Journal of Magnetic Resonance Imaging 29, 282–290.

Dai, W., Robson, P.M., Shankaranarayanan, A., Alsop, D.C., 2012. Reduced resolution transit delay prescan for quantitative continuous arterial spin labeling perfusion imaging. Magnetic Resonance in Medicine: Official Journal of the Society of Magnetic Resonance in Medicine/Society of Magnetic Resonance in Medicine 67, 1252–1265.

Detre, J.A., Rao, H., Wang, D.J., Chen, Y.F., Wang, Z., 2012. Applications of arterial spin labeled MRI in the brain. Journal of Magnetic Resonance Imaging: JMRI 35, 1026–1037.

Fernandez-Seara, M.A., Edlow, B.L., Hoang, A., Wang, J., Feinberg, D.A., Detre, J.A., 2008. Minimizing acquisition time of arterial spin labeling at 3 T. Magnetic Resonance in Medicine 59, 1467–1471.

Gunther, M., Bock, M., Schad, L.R., 2001. Arterial spin labeling in combination with a look-locker sampling strategy: inflow turbo-sampling EPI-FAIR (ITS-FAIR). Magnetic Resonance in Medicine 46, 974–984.

Gunther, M., Oshio, K., Feinberg, D.A., 2005. Single-shot 3D imaging techniques improve arterial spin labeling perfusion measurements. Magnetic Resonance in Medicine 54, 491–498.

Hernandez, D.A., Bokkers, R.P., Mirasol, R.V., Luby, M., Henning, E.C., Merino, J.G., Warach, S., Latour, L.L., 2012. Pseudocontinuous arterial spin labeling quantifies relative cerebral blood flow in acute stroke. Stroke; A Journal of Cerebral Circulation 43, 753–758.

Law, M., Young, R., Babb, J., Rad, M., Sasaki, T., Zagzag, D., Johnson, G., 2006. Comparing perfusion metrics obtained from a single compartment versus pharmacokinetic modeling methods using dynamic susceptibility contrast-enhanced perfusion MR imaging with glioma grade. AJNR. American Journal of Neuroradiology 27, 1975–1982.

MacIntosh, B.J., Lindsay, A.C., Kylintireas, I., Kuker, W., Gunther, M., Robson, M.D., Kennedy, J., Choudhury, R.P., Jezzard, P., 2010. Multiple inflow pulsed arterial spin-labeling reveals delays in the arterial arrival time in minor stroke and transient ischemic attack. AJNR. American Journal of Neuroradiology 31, 1892–1894.

Nael, K., Meshksar, A., Liebeskind, D.S., Wang, D.J., Ellingson, B.M., Salamon, N., Villablanca, J.P., 2013. Periprocedural arterial spin labeling and dynamic susceptibility contrast perfusion in detection of cerebral blood flow in patients with acute ischemic syndrome. Stroke; A Journal of Cerebral Circulation 44, 664–670.

Qiu, D., Straka, M., Zun, Z., Bammer, R., Moseley, M.E., Zaharchuk, G., 2012. CBF measurements using multidelay pseudocontinuous and velocity-selective arterial spin labeling in patients with long arterial transit delays: comparison with xenon CT CBF. Journal of Magnetic Resonance Imaging 36, 110–119.

Tatu, L., Moulin, T., Bogousslavsky, J., Duvernoy, H., 1998. Arterial territories of the human brain: cerebral hemispheres. Neurology 50, 1699–1708.

Wang, D.J., Alger, J.R., Qiao, J.X., Hao, Q., Hou, S., Fiaz, R., Gunther, M., Pope, W.B., Saver, J.L., Salamon, N., Liebeskind, D.S., 2012. The value of arterial spin-labeled perfusion imaging in acute ischemic stroke: comparison with dynamic susceptibility contrast-enhanced MRI. Stroke 43, 1018–1024.

Wolf, R.L., Alsop, D.C., McGarvey, M.L., Maldjian, J.A., Wang, J., Detre, J.A., 2003. Susceptibility contrast and arterial spin labeled perfusion MRI in cerebrovascular disease. Journal of Neuroimaging 13, 17–27.

Wu, O., Ostergaard, L., Weisskoff, R.M., Benner, T., Rosen, B.R., Sorensen, A.G., 2003. Tracer arrival timing-insensitive technique for estimating flow in MR perfusion-weighted imaging using singular value decomposition with a block-circulant deconvolution matrix. Magnetic Resonance in Medicine: Official Journal of the Society of Magnetic Resonance in Medicine/Society of Magnetic Resonance in Medicine 50, 164–174.

Zaharchuk, G., 2011. Arterial spin label imaging of acute ischemic stroke and transient ischemic attack. Neuroimaging Clinics of North America 21, 285–301.

Zaharchuk, G., El Mogy, I.S., Fischbein, N.J., Albers, G.W., 2012. Comparison of arterial spin labeling and bolus perfusion-weighted imaging for detecting mismatch in acute stroke. Stroke; A Journal of Cerebral Circulation 43, 1843–1848.